

Batch and circulated fluidized bed adsorption of nickel ions on algae: equilibrium, thermodynamic and mass transfer studies

Ahmed A. Mohammed, Aya Abbas Najim*

Department of Environmental Engineering, College of Engineering, University of Baghdad, Baghdad, Iraq, Tel. +9647901139275; emails: ayaaabbas@yahoo.com (A.A. Najim), ahmed.abedm@yahoo.com (A.A. Mohammed)

Received 31 October 2019; Accepted 12 May 2020

ABSTRACT

In this study, the biosorption potential of algae mixture (80% (*Chrysophyta*), 5% (*Cyanophyta*), and 14% (*Chlorophyta*)) to remove nickel ions from aqueous solution was investigated through batch and circulating fluidized bed (CFB). The effect of feed pH, dosage, the particle size of algae, and temperature in the batch mode was examined. The pH point zero charges (pH_{pzc}) was found equal to 5.8. The highest removal efficiency and mass transfer coefficient were 96.56% and 1.87×10^{-5} m/s, respectively. Also, results show that more than 79% adsorbed metal ion was desorbed by using 0.1 M HNO_3 in the first cycle. The effect of Ni(II) initial concentration, bed depth, and flow rate on the behavior of breakthrough curves was explained. The results showed that CFB has a better performance and lasts more than 5 h before the bed biomass exhausted in comparison with traditional fluidized bed, and the highest mass transfer coefficient (K_d) found equal to 2.118×10^{-5} m/s.

Keywords: Algae; Adsorption; Nickel; Fluidized bed; CFB; Mass transfer coefficient

1. Introduction

Metal contamination is considered to be one of the most worldwide and complex environmental matters today. Heavy metals are toxic pollutants, non-biodegradable, and stack in living tissues causing many defects and diseases [1]. Nickel ion a fundamental heavy metal for living organisms in admissible limits. Otherwise, when the permissible limits are exceeded then it is a famous environmental contaminant and its elimination is of major interest because nickel compounds are hazardous and also can cause bronchial asthma [2]. Nickel ions are found in the effluents of many industries such as mining and metallurgy of nickel, pigments and ceramic industries, accumulator manufacturing, zinc base casting, electroplating storage battery industries, used in silver refineries. The US Environmental Protection Agency (EPA) requires nickel not to exceed 0.015 mg/L in drinking water [3].

Various methods were used for wastewater treatment, among them, adsorption is an active and environmentally friendly alternative technique that can be carried out in batch and/or continuous mode. Biosorption a feature of certain types of inactive, dead biomass to join and concentrate contaminants from diluted solutions [4]. Among the most promising types of biosorbents studied are algae biomass, which has been reported to have high organic and inorganic binding capacities due to the existence of proteins, polysaccharides, or lipid on the cell wall structure. The cell wall containing carboxyl, amino, hydroxyl, and sulfate that refer to functional groups, which can act as binding sites for many contaminants [5].

The pharmaceutical industry, wastewater treatment with different substances, chemical industry, and food industry have been widely used fixed and fluidized bed reactors [6]. There are many disadvantages for the adsorption processes

* Corresponding author.

by fixed beds such as flow channels between the particles in the fixed beds always blocked by certain solid impurities in the raw extract causing higher pressure drop, dead zone. The motion of a fluid when it passes upward through a packed bed of granular particles, creates friction against the particles, tending to lift them. This lifting force increases as the velocity of the fluid increases until at some velocity, the fluid lifts all particles from contacting their neighbors to move freely. This mechanism called "Fluidization". Fluidized bed systems are popular and significant reactors in process engineering for the reason that good heat and mass transfer rate between the fluid and the particles and between the particles and the sidewall of the column [7]. Packed or fluidized bed adsorption system requires cyclic processes for adsorption, desorption, and washing which is a time-consuming and difficult process [8]. In recent years, the interest in the recovery of contaminants from large volumes of wastewater stream discharge from industrial and biological broths has increased, because of the progression in hereditary engineering, and concerns about recycling limited resources and environmental safety [8]. A new type of reactor known as gas, liquid, and solid circulating fluidized beds (GLSCFBs) has been used, in which the adsorbent is circulated between the downer and the riser [9]. GLSCFBs provided additional advantages to the traditional fluidized bed (TFB) which include, contact efficiency between liquid–solid is large, operated continuously because of adsorption and desorption work simultaneously that the particles circulated between two separate columns [10], reduced back mixing of phases, greater throughput and improved mass transfer owing to the higher velocity and uniform flow pattern [8]. The adsorption process occurs in the riser while the desorption process in the downer column. Lan et al. [10] studied the application of the LSCFB ion-exchange extraction system for the continuous protein recovery from cheese whey. According to the observed, the protein concentration in the liquid phase decreased with bed height in the down-comer. Higher overall protein recovery up to 90% was attained, with a lower concentration of protein in the effluent. To the best of our knowledge, circulating fluidized bed (CFB) has not yet been used in the removal of nickel ions from aqueous solution using algae biomass.

This work investigated the effects of environmental parameters such as pH, dosage, particle size, and temperature using mixed algae. Desorption and recovery experiments were performed in order to determine the ability of spent biosorbent for regeneration and reuse. The effectiveness of continuous removal of nickel(II) in CFB was studied by investigating the effects of bed height, the flow of liquid, and initial Ni(II) ions concentration. A comparison between the TFB and CFB was investigating. The mass transfer coefficient (K_t) was studied in both batch and GLSCFB mode.

2. Material and methods

A nickel nitrate hexahydrate (4.955 g) that has a molecular weight of 290.81 g/mol was dissolved in 1 L of distilled water to prepare (1,000) ppm of nickel (II), and the required concentrations were attained by dilution of the stock solution. 0.1 M of hydrochloric acid or sodium hydroxide was added to adjust the solution pH to the

desired value. A flame atomic absorption spectrophotometer AAS (Model: 210 VGP, USA) was used to determine the dissolved metal concentrations in the solution. Algae biomass were used in this work as biosorbent for nickel ions removal from aqueous solution. A mass of about 10 kg of algae was collected from the artificial irrigation canal near the college of engineering at the University of Baghdad in September of 2017. The water in this canal fed from the Tigris River. A sample about 0.5 kg of the algae that have been collected was analyzed for their species, genus, and percentage weight by using a microscope. These analyses were achieved according to the standard methods in the Biology Department, Ibn Al-Haitham College, University of Baghdad. The results showed that there are three divisions was dominated in this sample, 80 % golden-brown algae (*Chrysophyta*), 5% blue-green algae (*Cyanophyta*), and 14% green algae (*Chlorophyta*). Physical properties of the particles such as density, surface area, and porosity were measured and tabulated in Table 1. The values tabulated in Table 1 were important in the application of the fluidized bed. These measurements were performed in the laboratories of the Ministry of Oil/ Petroleum Development and Research Center.

2.1. Batch experiments




The conventional method used to determine the adsorbents point zero charges (pH_{pzc}) as cited by [11]. A 0.5 g biosorbent was mixed with 50 ml of 0.1 M NaCl solution in a 250 ml conical flask. Initial pH regimes (pH_i) were adjusted in a pH range of 2–10 using 0.1 M NaOH or HCl solutions [12]. The obtained suspensions were shaken for 24 h at 150 rpm in an incubator shaker (ISO 9001, Model: LSI-3016, NO.B110416002, Korea). The final pH of the solution was measured after the adsorbent was filtered. The final pH-initial pH was plotted versus initial pH, where the intersection point of the two curves determines the pH_{pzc} of the algae biomass. In order to reduce the cost of processing, desorption is the best choice that allows for reusing the adsorbent. The loaded biomass with an initial concentration of 100 ppm from the batch process about 1 after Ni(II) ions biosorption, were placed in 100 ml of (0.05 and 0.1 M) HNO_3 for 1 h. After the filtration procedure, the filtrate was analyzed for metal concentration. The residual algae after filtration washed with distilled water, and dried in an oven at 60°C to reuse again to adsorb Ni(II) in the next cycle, this procedure repeated five times. The uptake is calculated for each biomass weight using Eq. (1), the percentage of removal efficiency was calculated using Eq. (2) [13], and the eluting efficiency of the biosorbent (E_d) is expressed by Eq. (3) [14]:

$$q_e = \frac{(C_i - C_e)V}{m} \quad (1)$$

$$\% \text{ Removal efficiency} = \frac{C_i - C_e}{C_i} \times 100 \quad (2)$$

$$E_d (\%) = \frac{m_d}{m_{\text{ad}}} \times 100 \quad (3)$$

Table 1
Physical properties of algal biomass

Particle dim., mm	0.5 (1–0.25)	0.177 (0.25–0.125)	0.089 (0.125–0.063)
Parameter			
Bulk density (kg/m ³)	640.8	684.62	730.76
Real density (kg/m ³)	2,107.5	2,107.5	2,107.5
Surface area (m ² /g)	2.5807	2.6555	3.2403
Particle porosity (–)	0.696	0.675	0.653

where q_e is the amount of adsorbate adsorbed per mass of adsorbent, mg/g, C_i is the initial concentration, mg/L, C_e is the equilibrium concentration, mg/L, v is the volume of solution, L, m is the mass of sorbent, g, m_{ad} is the total adsorbed quantity of contaminants, mg/L, m_d is the contaminant mass desorbed, mg/L.

2.2. Continuous experiments

Fig. 1 illustrates a schematic diagram of gas, liquid, and solid circulated fluidized bed consisting of a riser (5 cm and 100 cm high) and a downer (15 cm and 80 cm high). A liquid–solid separator used to separate solids from the liquid was located at the top of the downer. The upper section diameter of the separator was 15 cm, and the bottom section of the separator was funnel-shaped. The major components of the GLSCFB system are shown in Fig. 1. Before

the operation, the downer is filled with desorption solution (in this case distilled water). Different weight of algae biomass was placed at the bottom of the riser as biosorbent. At operation, both the wastewater containing nickel ions was pumped into the bottom of the riser at constant flow rate passed through the distributor, and the air is supplied from the compressor at 250 cm³/min. Adsorption and fluidization phenomena occurred in the riser column and the three-phase (air, wastewater, and algae biomass) were transferred from the end of the riser to the three-phase separator where the air is separated to the atmosphere. The liquid-filled the cone part of the separator at low velocity. The angle of the cone ensure laminar flow and prevent any rapid mixing between the wastewater and the regeneration water. This will create a small interface region where the solid particles will pass through due to the gravity force. The particle will contact the regeneration water (distilled

1: Feeding tank, 2: Valve, 3: Pump, 4: Air compressor, 5: Solid circulating measuring device, 6: Flow meter of liquid, 7: Gas flow meter, 8: Distributer, 9: Solid-liquid separator, 10: Treated wastewater, 11: Distilled water for the downer, 12: Downer column, 13: Riser column, 14: Sampling port in the riser, 15: Sampling port in the downer, 16: Port to enter algae biomass.

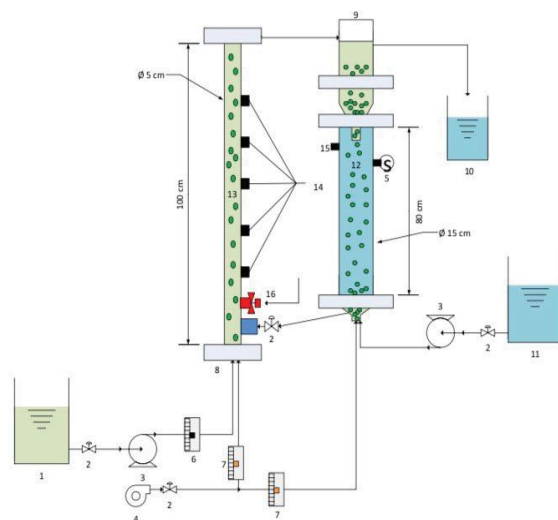


Fig. 1. Schematic diagram of the gas–liquid–solid circulating fluidized bed.

water) where desorption will occur and the particle will settle at the bottom of the regenerator (downer). Air is introduced at the bottom of the downer to generate mixing and increase the desorption of the particle. The valve located between the two columns will prevent the mixing between the wastewater and the regenerated water and accumulate the solid particles at the bottom of the downer. After a period of time, the valve is opened to recirculate the regenerated particle.

3. Results and discussion

3.1. Batch mode

3.1.1. Effect of experimental parameter

The solution pH is a significant issue impacting the subtraction of contaminants from aqueous solutions, affect the functional groups on the adsorbent surface, and determine the solubility of a contaminant in the aqueous medium [15]. The effect of pH on the Ni(II) removal percentage could be explained on the basis of the zero point charge (pH_{pzc}) of the biosorbent. The pH_{pzc} is the point at which the net charge of the adsorbent is zero. The pH_{pzc} is an important parameter that determines the linear range of pH sensitivity and then indicates the type of surface-active centers and the adsorption ability of the surface [16,17]. The pH_{pzc} of algae biomass was found equal to 5.8 (Fig. 2), where the electrostatic repulsion between adsorbent molecules is minimized. The effect of solution pH on the removal efficiency of Ni(II) ions on the sorbent was examined by adjusting the pH in the range of 3–8. The initial pH values were investigated up to 8.0 since insoluble nickel hydroxide starts to precipitate from solution at higher pH values, making true sorption studies impossible [18]. Fig. 3 shows the effect of pH on the removal percentage, from this figure it can be noticed that the removal efficiency increases with increasing the pH. The minimum removal efficiency was observed at pH = 3.0, this action may be owing to the existence of higher H^+ ion concentration [19]. In opposite with the increase in pH 3.0–6.0 the surface area becomes more negatively charged thus facilitating greater metal removal by algal biomass, due to the absence of hydrogen ions and which leading to increase the ability to establish links between metal cations and algae biomass

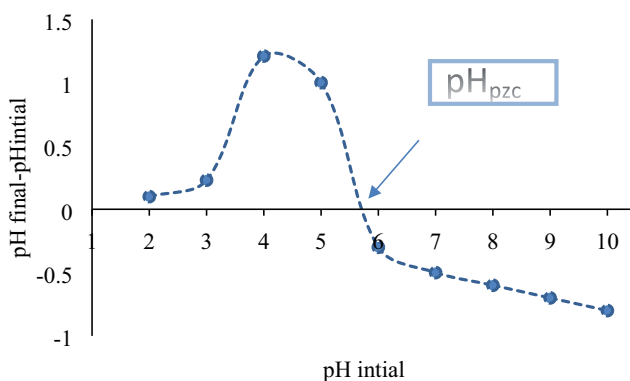


Fig. 2. Point zero charge of algae biomass ($m = 0.5$ g/50 ml of 0.1 M NaCl; 25°C; $T = 24$ h, 89 μ m, and 150 rpm).

[20]. At high pH 7.0–8.0, the percentage removal decreases, this decrease could be associated with the repulsion between the negative charge of anionic species in solution and negative surface charge of the sorbents, or some active groups on the adsorbent surface may be less protonated according to the effect of zeta potential [21].

The effect of varying the adsorbent dose (mass) on the adsorption of nickel ions is shown in Fig. 4. The biomass dosage is a significant parameter used to determine the capacity of biosorbent for specific initial concentration, it is one of the most essential factors that effected the biosorption process [22]. In this work, various amounts of algae biomass (0.2–2 g/100 ml) were used. By increasing the amount of algal biomass, the pollutants may be fully adsorbed or reach an equilibrium state when reaching a plateau at a fixed concentration of each pollutant [23]. It is clearly seen that the removal efficiency of Ni(II) ions increases from 40.82 to 90.63%, as the algae mass increases from 0.2 to 1 g for Ni(II) ions. After some point (above 1 g for Ni(II)), the biosorption capacity was unchanged owing to a screen effect between biomass, this created a block of the biomass functional groups. Overloading of biomass does not increase

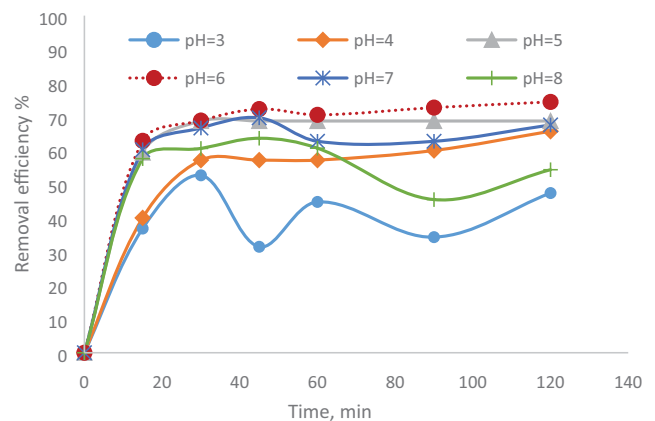


Fig. 3. The effect of pH with time on the removal efficiency of Ni(II) ($m = 0.5$ g/100 ml; 25°C; $C_i = 35$ mg/L; speed = 200 rpm; 89 μ m).

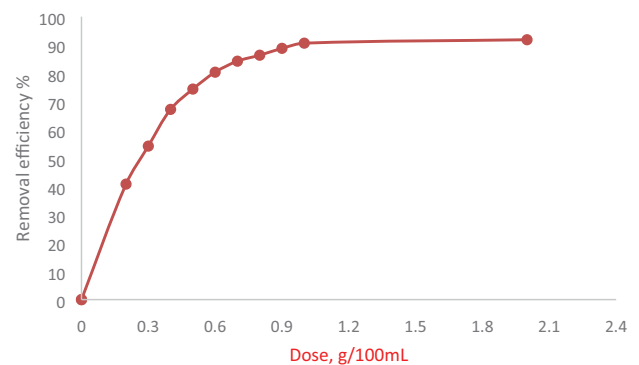


Fig. 4. Effect of biosorbent dose on the percentage removal of nickel ions by algae biomass (pH 6, 25°C; $C_i = 35$ mg/L; speed = 200 rpm; 89 μ m; time = 120 min).

contaminant removal efficiency rather it would increase the cost of the process, due to the fact that fixed initial concentration led to the unsaturated active site on biomass surface and an increase in the biomass concentrations cause particle aggregation, while at low biomass doses, the surfaces became saturated faster because all locations were totally exposed to the pollutant, a higher value of q_e [24].

The surface area of the sorbent is an important parameter for sorption. Fig. 5 shows the relationship between the particle size of the sorbent and the removal efficiency of Nickel ions. The results show that the removal efficiency increased with the decrease in particle size from 500 to 89 μm . The higher sorption level accomplished by the smallest size of particle may be due to the fact that smaller particle size gives larger surface areas and exhibit rapid adsorption than that of sorbents with the lower surface area. The observed results agree with Arunakumara et al. [25]. The surface area of used particles are tabulated in Table 1.

3.1.2. Effect of temperature and thermodynamic parameters

The temperature has a vigorous effect on the adsorption process as it can influence the process by an increase or decrease in the amount of adsorption [22]. The results are plotted in Fig. 6, which show the adsorption efficiency of Ni(II) ions and onto algae biomass at five different temperatures of 20°C, 25°C, 30°C, 35°C and 40°C, from this figure, it can be seen that removal efficiency increase with increasing temperature, signifying the endothermic nature of the process. The removal efficiency increases as temperature increases till it reaches 40°C. At higher temperatures (45°C

and 50°C), the texture of biomass was changed, damage and reduce the number of functional groups, that is why the temperature was limited to 40°C.

Thermodynamic parameters were obtained by varying temperature conditions over the range of 20°C–40°C, at an initial concentration of 35 mg/L for Ni(II) ions and optimum: pH and dosage. The thermodynamic parameter values such as ΔH° , ΔG° , ΔS° , E_a , and S^* , describing Ni(II) ions uptake by algae biomass are calculated from equations (4–8) [26] and tabulated in Table 2. The values of enthalpy and entropy were achieved from the slope and intercept of $\ln K_c$ vs. $1/T$ (figure not shown).

$$\ln K_c = \left(\frac{\Delta S^\circ}{R} \right) - \left(\frac{\Delta H^\circ}{RT} \right) \tag{4}$$

$$\Delta G^\circ = \Delta H^\circ - \Delta S^\circ T \tag{5}$$

$$KC = \frac{C_{ad}}{C_e} \tag{6}$$

$$S^* = (1 - \theta) \exp\left(-\frac{E_a}{RT}\right) \tag{7}$$

$$\theta = \left(1 - \frac{C_e}{C_i}\right) \tag{8}$$

where K_c stands for the equilibrium constant, C_{ad} stands for the adsorbed concentration of Ni(II) on the adsorbent per

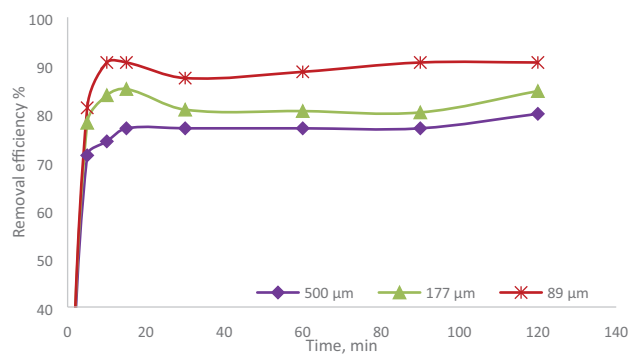


Fig. 5. Effect of sorbent particle size with time on the removal efficiency of Ni(II) (pH 6; $m = 1$ g; 25°C, $C_i = 35$ mg/L, at speed = 200 rpm).

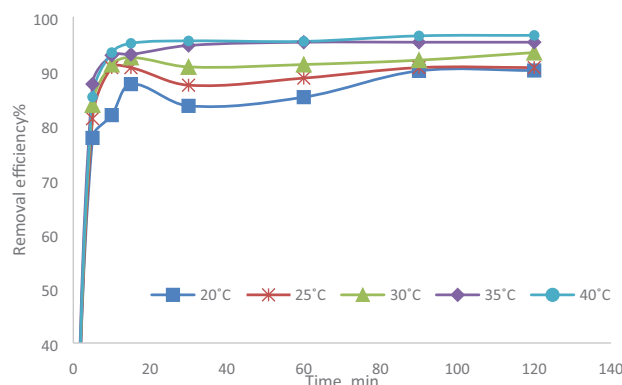


Fig. 6. Effect of temperature with time on the removal efficiency of Ni(II) (pH 6; $m = 1$ g; $C_i = 35$ mg/L; 89 μm ; speed = 200 rpm).

Table 2
Thermodynamic parameters for the sorption of nickel ions on algae biomass

T (K)	ΔG° (kJ/mol)	ΔS° (J/mol K)	ΔH° (KJ/mol)	E_a (kJ/mol)	S^*
293	-5.0844				
298	-5.9476				
303	-6.8108	172.64	45.4992	42.623	2.799×10^{-9}
308	-7.6740				
313	-8.5372				

liter of the solution at equilibrium (mg L^{-1}), C_e is the equilibrium concentration of Ni(II) in the solution (mg L^{-1}), ΔH° stands for the biosorption process enthalpy (kJ/mol), R stands for the universal gas constant (8.314 J/mol K), ΔS° stands for the biosorption process entropy (J/K mol), ΔG° stands for the Gibbs free energy of biosorption (kJ/mol), T stands for the solution temperature (K), θ is surface coverage, S^* is sticking probability, and E_a is the activation energy.

ΔH° and E_a positive values reveal the adsorption is endothermic and higher solution temperature favors Ni(II) ions removal by algae biomass. Similarly, the ΔS° values are positive, indicating increasing in randomness at the solid/solution interface during their sorption. At all studied temperatures, the negative values of ΔG° suggested the spontaneous of the sorption process with a high affinity of nickel (II) ions to algae biomass. The value of sticking probability (S^*) is found very close to zero indicates that the biosorption process follows chemisorption.

3.1.3. Desorption study

The recyclability of an adsorbent is of fundamental importance in industrial practice for pollutant removal from wastewater [27]. Desorption of the adsorbed Ni(II) ions from the tested algae biomass were studied in a batch system. The metal ion onto biosorbent was eluted with various concentrations of nitric acid. More than 79% of adsorbed metal ion were desorbed from the biosorbent by using 0.1 M HNO_3 in the first cycle. If desorbent achieves the assigned standards, it is possible to regenerate the biomass in order to use in another biosorption cycle and metal ions recover in the form of a concentrated solution. In order to show the reusability of algae biomass, adsorption–desorption cycle of pollutants was frequented five times by using the same preparations. The recovery percentages using two concentrations of HNO_3 from algae biomass were calculated from Eq. (3). Fig. 7 shows that with increasing the nitric acid concentration from 0.05 to 0.1 M, the amount of metal recovery increase from 42% to 79.82%, and algae biomass could be repeatedly used in metal biosorption studies without detectable losses in their initial

biosorption capacities. Not only the recovery efficiency improved when increasing the concentration of nitric acid, but also the biosorption in the second cycle increased from 64.3% to 75.8% for nickel ions. Nitric acid was used for this purpose to recover the same salts used at the first time, and the reason for using acid elution is due to the fact that most biosorption exhibit an ion-exchange mechanism for cations and thus increasing the acidity of metals loaded algae lead to leaching of metals ions from biosorbent [28].

3.2. GLSCFB mode

Fluidization is a process in which the upward flow of a fluid suspends a bed of particles [29], and the minimum fluidization velocity is the velocity required to begin the fluidization at which the weight of particles gravitational force equals the drag on the particles from the rising fluids [30]. Once the bed is fluidized, the pressure drop across the bed remains constant, but the bed height continues to increase with increasing flow. The minimum fluidization velocity (U_{mf}) was found experimentally equal to 0.76 mm/s for a particle size diameter of 0.5 mm. It is important to be able to establish the relationship between the superficial liquid velocity (U) and the bed voidage (ϵ) [31]. The voidage (ϵ) of fluidized algal biomass was found experimentally using Eq. (9) which has a value of 0.85.

$$\epsilon = \frac{V_\epsilon}{V_b} = \frac{V_b - V_p}{V_b} = 1 - \frac{V_p}{V_b} = 1 - \frac{m_p}{\rho_p \cdot v_b} = 1 - \frac{m_p}{\rho_p \cdot A \cdot h_{mf}} \quad (9)$$

where ϵ is the bed voidage (-), V_ϵ is the void volume, m^3 , V_b is the Volume of bed, m^3 , m_p is the mass of particles, kg , ρ_p is the real density of particles, kg/m^3 , V_b is the volume of bed, m^3 , A is the cross-section area of the column, m^2 , h_{mf} is the fluidized bed height, m .

3.2.1. Effect of liquid flow rate

The fluid flow rate is a major parameter in the design of the biosorption column especially fluidized bed reactor due to its effect on the contact time between the particles

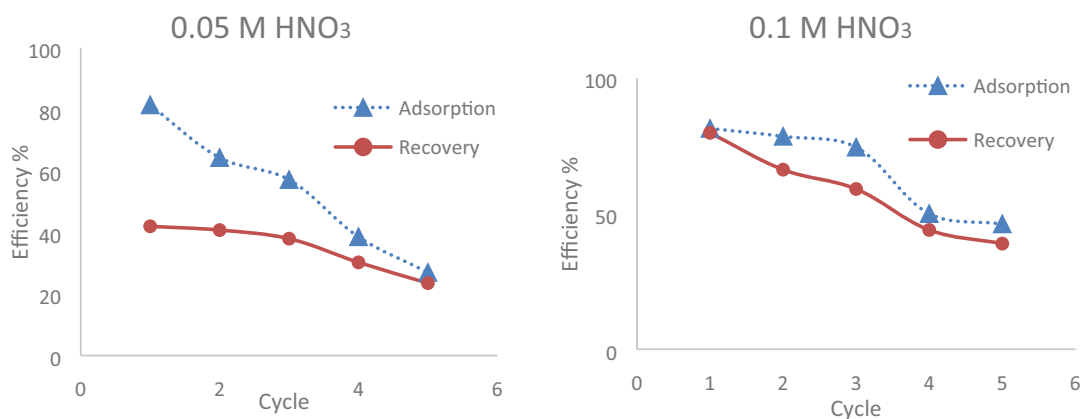


Fig. 7. Five cycle of adsorption-desorption of Ni(II) ions with two different concentrations of HNO_3 (pH 6; $m = 1 \text{ g}$; $C_i = 100 \text{ mg/L}$; $89 \mu\text{m}$; speed = 200 rpm; time = 120 min; desorption time = 60 min).

and contaminant solution. Increased the volume of wastewater flowing through the same units results in reduced residence time, thereby lowering the removal efficiency of the system. This causes the effluent to have higher than usual concentrations of pollutants [29]. The results of the effect of the liquid flow rate on the removal efficiency of nickel ions are plotted in Fig. 8, which shows that the ratio of C_e/C_i rises from 0.39 to 0.8 as the liquid flow rate increase from 6 to 12 L/h. Pollutant concentration in the liquid phase increase throughout the column with the increase in liquid flow rate (velocity of liquid). This can be explained in term of residence time, the residence time of the liquid phase decreases with an increase in liquid velocity. A shorter residence time results in reduced time for adsorption and higher pollutant concentration in the raffinate stream. These results agree with that obtained by [8,32].

3.2.2. Effect of bed height

Fig. 9 shows the effect of bed height on the biosorption process, $C_i = 50$ ppm, $d_p = 500$ μm , liquid flow rate = 6 L/h,

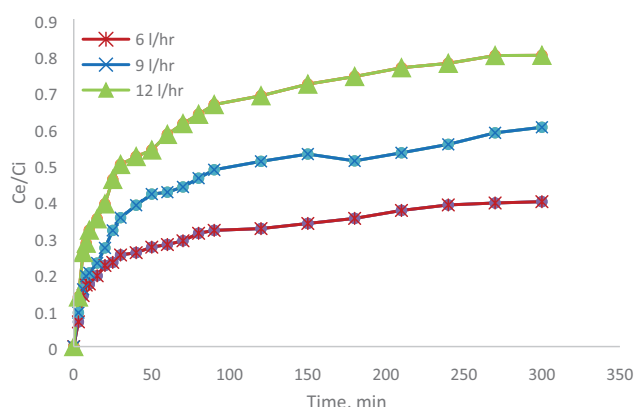


Fig. 8. Effect of flow rate on the removal of Ni(II) at initial conditions 100 g (8 cm), pH 6, 50 mg/L, and airflow rate 250 cm³/min.

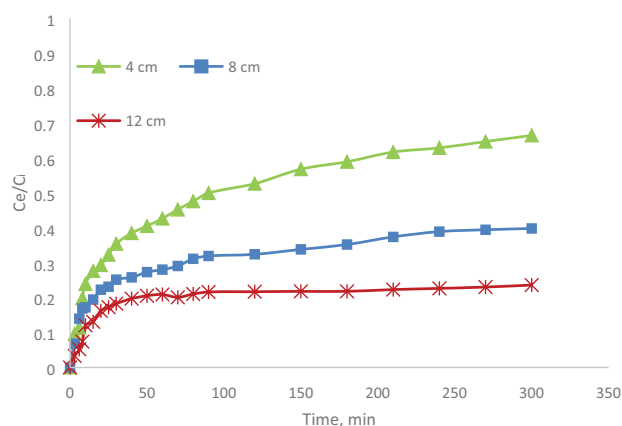


Fig. 9. Effect of bed height at initial conditions pH 6, 50 ppm, 6 L/h, and airflow rate 250 cm³/min on the removal of Ni(II) ions.

airflow rate = 250 cm³/min, and bed weight 50, 100 and 150 g (corresponding to static bed heights 4, 8 and 12 cm). It can be seen from this figure, with increasing bed height, the time needed to reach equilibrium increased. This is due to large contact time occurred between contaminants and particles at high bed height. Smaller bed heights will be saturated in less time; this shows that at smaller bed height the effluent adsorbate concentration ratio increases more rapidly than that for higher bed height. Also, an increase in the bed height will increase the surface area or biosorption sites which improve the biosorption process. These results agree with that obtained by [10,33]. An increase in the bed height results in an increase of the residence time of particles in the bed [34].

3.2.3. Effect of initial concentration

Fig. 10 shows the effect of initial concentration in the feed on the biosorption of nickel ions. When feed concentration increased from 50 to 150 mg/L for a nickel. The concentration in the raffinate stream increased, this is due to an increase in the concentration gradient [8]. In low initial pollutant concentration, the diffusion rate will take a longer time to reach saturation. It is also clear that the adsorption capacity increases, when the influent concentration increases. This is due to a high concentration difference between the bulk solution and the concentration of the solute on the solid phase. This will increase the rate of mass transfer of solute to attach a free site (s) on the solid phase. The driving force for adsorption is the concentration difference between the solute on the adsorbent and in the solution. On the other hand, the saturation of the bed is faster and the slope of the breakthrough curve is higher when the initial concentration is high.

3.2.4. Comparison between TFB and circulated fluidized bed

The behavior of breakthrough curves of TFB (conventional) and the CFB are investigated at 50 mg/L as initial

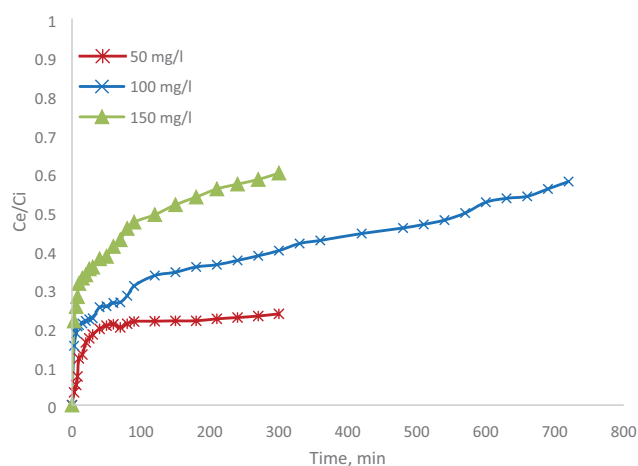


Fig. 10. Effect of initial concentrations on the removal of Ni(II) ions at initial conditions pH 6, 150 g (12 cm), 6 L/h, and 250 cm³/min.

Ni(II) concentration, 100 g (8 cm) for bed height, 6 L/h as liquid volumetric flow rate, and 250 cm³/min as gas flow rate. The results obtained are shown in Fig. 11, that show the efficiency of CFB on the removal of Ni(II) ion. So the CFB has a better result and lasts for more than 5 h before the biomass exhausted. In a CFB, solid particles are circulated between the riser and the downer at higher velocities compared to conventional fluidized beds, which leads to better-contacting efficiency between phases, and higher mass transfer can be achieved with CFBs, which makes this type of reactor more preferable over the conventional fluidized beds. It has also been reported that the GLSCFB provides higher gas holdup, more uniform bubble sizes, better inter-phase contact, and more efficient heat transfer into or out of the bed [35]. For some gas–liquid–solid reaction systems, solid adsorbent loses their activity due to deposition of metal and coke on their surfaces and needs regeneration outside the bed. By using an accompanying downer as a regenerator, both reaction and regeneration of the catalysts can be coupled with a continuous circulating operation [35,36]. The liquid velocity is not enough to entrain the particles and wash them out of the column in conventional fluidization, while in a circulated fluidized bed, the particles were carried to the top of the column by using high liquid velocity and then return them to the bottom by a recycle line or column [29].

4. Mass transfer coefficient

4.1. Batch mode

The external mass transfer coefficient (K_L) in a batch system was determined at different biomass concentrations and particle sizes using Eq. (10) [37]. The values of the mass transfer coefficient are tabulated in Tables 3 and 4. From these tubules, the mass transfer coefficient decrease with increasing the biomass dose, and decrease with decreasing the particle size.

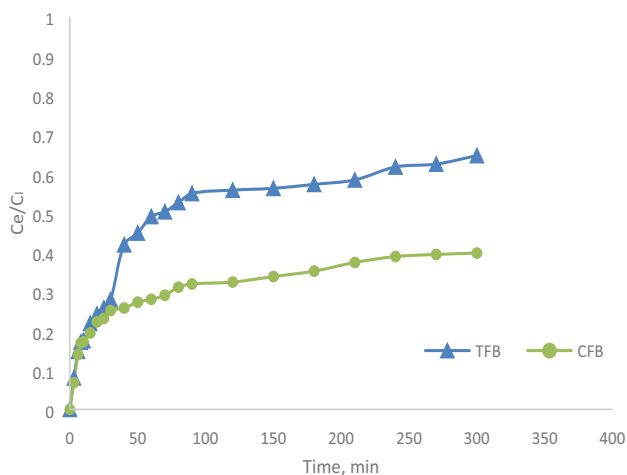


Fig. 11. Traditional fluidized bed (TFB) vs. CFB for the removal of Ni(II) ions at initial conditions 6 L/h as flow rate, 8 cm as bed height, 50 ppm as initial concentration, and 250 cm³/min as gas flow rate.

$$K_L = -\frac{d_p \cdot \rho_p \cdot V_L}{3m \cdot t} \ln\left(\frac{C_e}{C_i}\right) \quad 0 < \frac{C_e}{C_i} < 1 \quad (10)$$

4.2. Continuous mode

The magnitude of mass transfer is represented by the values of gas–liquid mass transfer coefficient (K_L). It acts as a function of superficial gas and liquid velocity. Liquid velocity has powerless effects on oxygen transfer, but gas velocity affected K_L positively [38]. Mass transfer is influenced by gas holdup and liquid holdup. Generalized correlations were proposed by several authors to predict the mass transfer coefficient K_L in continuous systems. The calculated K_L values using these correlations are listed in Table 5, these values were calculated for different operating conditions. In which the Schmidt number ($Sc = \nu/D_m$) is calculated using the liquid kinematic viscosity, ν (m²/s), and the liquid phase diffusivity, D_m (m²/s). The diffusivity of each pollutant was calculated using Eq. (6). The diffusivity was 4.136×10^{-10} m²/s. The Re_p values of 0.5 mm diameter particles are equal 0.476, 0.714 and 0.951 for 6, 9 and 12 L/h, respectively. From Table 5, the mass transfer coefficient values were increased from 3.494×10^{-6} to 4.920×10^{-6} (the first correlation) and from 1.504×10^{-5} to 2.118×10^{-5} (the second correlation) when the flow rate of the liquid increased from 6 to 12 L/h. The reason behind this action is that the change in flow rate will affect the film diffusion, but not the intra-particle diffusion. The higher the flow rate the smaller the film resistance to mass transfer and larger K_L values.

$$D_m = 2.74 \times 10^{-9} (\text{Mwt})^{-1/3} \quad (11)$$

Table 3
Mass transfer coefficient at different biomass dosage

Mass (g/100 ml)	K_L (m/s)
0.2	2.28×10^{-6}
0.3	2.26×10^{-6}
0.4	2.42×10^{-6}
0.5	2.37×10^{-6}
0.6	2.36×10^{-6}
0.7	2.29×10^{-6}
0.8	2.163×10^{-6}
0.9	2.11×10^{-6}
1	2.05×10^{-6}
2	1.09×10^{-6}

Table 4
Mass transfer coefficient at different particle size diameter

Particle size, μm	K_L (m/s)
1,304	1.87×10^{-5}
500	7.85×10^{-6}
177	3.24×10^{-6}
89	2.056×10^{-6}

Table 5
Calculated K_L values of Ni(II) ions at different flow rate

Correlation (Bartelmus [39])	Ni(II)					
	$Sh_z = K_L \cdot \eta_z / D_m$			K_L (m/s)		
	6 L/h	9 L/h	12 L/h	6 L/h	9 L/h	12 L/h
$\frac{Sh_z}{Sc^{0.33}} = 2.269 (Re_{zL})^{0.494} (Re_{zg})^{0.178} Ga^{-0.276}$	0.366	0.447	0.515	3.494×10^{-6}	4.268×10^{-6}	4.920×10^{-6}
$\frac{Sh_z}{Sc^{0.33}} = (1.19 + 0.0072 Re_{zg})^{1.1} \times (Re_{zL})^{0.494} Ga^{-0.22}$	1.575	1.925	2.218	1.504×10^{-5}	1.838×10^{-5}	2.118×10^{-5}

5. Conclusions

The results indicated that algae biomass could be used as an efficient biosorbent material for the removal of nickel ions from aqueous solution. The optimum pH, dose, and particle size were pH 6, 1 g/100 ml, and 89 μm in the batch mode. The pH_{pzc} was 5.8. At range (293–313) K, thermodynamic parameters (ΔG° , ΔH° , ΔS° , E_a and S^*) were studied and the results suggested that biosorption process was a spontaneous reaction, an endothermic in nature, and the biosorption process follows chemisorption. The maximum removal efficiency achieved was 96.56%. Results show that adsorption–desorption process lasts for five cycles before losing its efficiency and the recovery efficiency increased from 42% to 79.82% when the concentration of nitric acid increased from 0.05 to 0.1 M. The mass transfer coefficient in the batch mode decrease with increasing the biomass dose and decrease with decrease the biomass particle size in batch mode while increasing with increase the liquid flow rate in the continuous mode. The GLSCFB show better performance and last more than 5 h before the bed of biomass exhausted and the value of C_f/C_i was 0.65 and 0.39 for TFB and CFB, respectively after 5 h operation.

Nomenclature

- A — Cross section area of the column, m^2
- a — External surface area of packing per unit column volume, m^2/m^3
- C_e — Equilibrium concentration, mg/L
- C_i — Initial concentration, mg/L
- D — Bed diameter, m
- D_m — Diffusivity coefficient, m^2/s
- d_p — Particle diameter, m
- E_a — Activation energy, kJ/mol
- Ga — Galileo number, $d_p^3 \rho_L^2 g / \mu_L^2$
- ΔG° — Gibbs free energy change, kJ/mol
- h_{mf} — Fluidized bed height, m
- ΔH° — Enthalpy changes, kJ/mol
- K_C — The equilibrium constant
- K_L — Mass transfer coefficient, m/s
- m — The mass of sorbent, g
- m_{ad} — Total adsorbed quantity, mg/L
- m_d — The mass desorbed, mg/L
- Mwt — Molecular weight
- q_e — Amount of adsorbate adsorbed per mass of adsorbent, mg/g

- R — Removal efficiency, %
- R — Density ratio, $1 - \rho_p / \rho_L$
- R — The universal gas constant (8.314), J/mol K
- Re_p — Reynolds number for particle, $U d \rho_l / \mu_l$
- Re_{zg} — Modified Reynolds number for gas, $U_g \rho_g / a \mu_g$
- Re_L — Reynolds number for liquid, $d_p U_L \rho_L / \mu_L$
- Re_{zL} — Modified Reynolds number, Re_L / ϵ_L
- Sc — Schmidt number, $\mu / \rho D_m$
- Sh — Sherwood number, $K_L d / D_m$
- Sh_z — Modified Sherwood number, $K_L \eta_z / D_m$
- S^* — Sticking probability
- ΔS° — Entropy changes, J/mol K
- T — Temperature, K
- t — Time, min
- U_L — Superficial liquid velocity, m/s
- U — Gas velocity, m/s
- U_{mf}^g — Minimum fluidization velocity, m/s
- V_L — volume of wastewater solution, m^3
- V_b — Volume of bed, m^3
- V_p — Volume of particles, m^3
- V^p — Void volume, m^3
- V^ϵ — Void volume, m^3
- ρ_l — Liquid density, kg/m^3
- ρ_s — Real density of particles, kg/m^3
- ρ_{bulk} — Bulk density of particles, kg/m^3
- ρ_G — Density of gas, kg/m^3
- ϵ — Bed voidage
- ϵ_G — Gas holdup
- ϵ_L — Liquid holdup
- ϵ_s — Solid holdup
- ν — Kinematic viscosity, m^2/s
- μ_g — Viscosity of gas, Pa s
- μ_L — Viscosity of liquid, Pa s
- η_z — Equivalent film thickness $(\mu_l^2 / g \rho_l^2)^{1/3}$, m
- θ — Surface coverage

References

- [1] M. Akbari, A. Hallajisani, A.R. Keshtkar, H. Shahbeig, S.A. Ghorbanian, Equilibrium and kinetic study and modeling of Cu(II) and Co(II) synergistic biosorption from Cu(II)-Co(II) single and binary mixtures on brown algae *C. indica*, J. Environ. Chem. Eng., 3 (2015) 140–149.
- [2] M. Zaheer Aslam, N. Ramzan, S. Naveed, N. Feroze, Ni(II) removal by biosorption using *Ficus religiosa* (peepal) leaves, J. Chil. Chem. Soc., 55 (2010) 81–84.
- [3] Y. Hannachi, A. Hannachi, The efficiency of the flotation technique for the removal of nickel ions from aqueous solution, Desal. Water Treat., 6 (2009) 299–306.

- [4] H. Pahlavanzadeh, A.R. Keshtkar, J. Safdari, Z. Abadi, Biosorption of nickel(II) from aqueous solution by brown algae: equilibrium, dynamic and thermodynamic studies, *J. Hazard. Mater.*, 175 (2010) 304–310.
- [5] T.A. Davis, B. Volesky, A. Mucci, A review of the biochemistry of heavy metal biosorption by brown algae, *Water Res.*, 37 (2003) 4311–4330.
- [6] Y.G. Park, S.Y. Cho, S.J. Kim, G.B. Lee, B.H. Kim, S.-J. Park, Mass transfer in semi-fluidized and fluidized ion-exchange beds, *Environ. Eng. Res.*, 4 (1999) 71–80.
- [7] A.H. Sulaymon, A.A. Mohammed, T.J. Al-Musawi, Column biosorption of lead, cadmium, copper, and arsenic ions onto algae, *J. Bioprocess. Biotech.*, 3 (2013) 2.
- [8] J. Mazumder, J. Zhu, A.S. Bassi, A.K. Ray, Modeling and simulation of liquid–solid circulating fluidized bed ion exchange system for continuous protein recovery, *Biotechnol. Bioeng.*, 104 (2009) 111–126.
- [9] Z. Liu, M. Vatanakul, L. Jia, Y. Zheng, Hydrodynamics and mass transfer in gas–liquid–solid circulating fluidized beds, *Chem. Eng. Technol.*, 26 (2003) 1247–1253.
- [10] Q. Lan, A. Bassi, J.X.J. Zhu, A. Margaritis, Continuous protein recovery from whey using liquid–solid circulating fluidized bed ion-exchange extraction, *Biotechnol. Bioeng.*, 78 (2002) 157–163.
- [11] A. Mohseni-Bandpi, T.J. Al-Musawi, E. Ghahramani, M. Zarrabi, S. Mohebi, S.A. Vahed, Improvement of zeolite adsorption capacity for cephalixin by coating with magnetic Fe₃O₄ nanoparticles, *J. Mol. Liq.*, 218 (2016) 615–624.
- [12] A. Celekli, M. Yavuzatmaca, H. Bozkurt, Kinetic and equilibrium studies on the adsorption of reactive red 120 from aqueous solution on *Spirogyra majuscula*, *Chem. Eng. J.*, 152 (2009) 139–145.
- [13] P.R. Puranik, J.M. Modak, K.M. Paknikar, A comparative study of the mass transfer kinetics of metal biosorption by microbial biomass, *Hydrometallurgy*, 52 (1999) 189–197.
- [14] S.R. Pilli, V.V. Goud, K. Mohanty, Biosorption of Cr(VI) on immobilized *Hydrilla verticillata* in a continuous up-flow packed bed: prediction of kinetic parameters and breakthrough curves, *Desal. Water Treat.*, 50 (2012) 115–124.
- [15] A.A. Mohammed, S.S. Isra'a, Bentonite coated with magnetite Fe₃O₄ nanoparticles as a novel adsorbent for copper (II) ions removal from water/wastewater, *Environ. Technol. Innovation*, 10 (2018) 162–174.
- [16] A.E. Pirbazari, E. Saberikhah, M. Badrouh, M.S. Emami, Alkali treated foumanat tea waste as an efficient adsorbent for methylene blue adsorption from aqueous solution, *Water Res. Ind.*, 6 (2014) 64–80.
- [17] A.A. Mohammed, T.J. Al-Musawi, S.L. Kareem, M. Zarrabi, A.M. Al-Ma'abreh, Simultaneous adsorption of tetracycline, amoxicillin, and ciprofloxacin by pistachio shell powder coated with zinc oxide nanoparticles, *Arabian J. Chem.*, 13 (2020) 4629–4643.
- [18] A. Lopez, N. Lazaro, J.M. Priego, A.M. Marques, Effect of pH on the biosorption of nickel and other heavy metals by *Pseudomonas fluorescens* 4F39, *J. Ind. Microbiol. Biotechnol.*, 24 (2000) 146–151.
- [19] Y.B. Onundi, A.A. Mamun, M.F. Al Khatib, Y.M. Ahmed, Adsorption of copper, nickel and lead ions from synthetic semiconductor industrial wastewater by palm shell activated carbon, *Int. J. Environ. Sci. Technol.*, 7 (2010) 751–758.
- [20] A.K. Zeraatkar, H. Ahmadzadeh, A.F. Talebi, N.R. Moheimani, M.P. McHenry, Potential use of algae for heavy metal bioremediation, a critical review, *J. Environ. Manage.*, 181 (2016) 817–831.
- [21] S. Kalyani, P.S. Rao, A. Krishnaiah, Removal of nickel (II) from aqueous solutions using marine macroalgae as the sorbing biomass, *Chemosphere*, 57 (2004) 1225–1229.
- [22] R. Palaniswamy, C. Veluchamy, Biosorption of heavy metals by *Spirulina platensis* from electroplating industrial effluent, *Environ. Sci. Ind. J.*, 13 (2017) 139.
- [23] R.K. Gautam, A. Mudhoo, M.C. Chattopadhyaya, Kinetic, equilibrium, thermodynamic studies and spectroscopic analysis of Alizarin red S removal by mustard husk, *J. Environ. Chem. Eng.*, 1 (2013) 1283–1291.
- [24] H.T. Tran, N.D. Vu, M. Matsukawa, M. Okajima, T. Kaneko, K. Ohki, S. Yoshikawa, Heavy metal biosorption from aqueous solutions by algae inhabiting rice paddies in Vietnam, *J. Environ. Chem. Eng.*, 4 (2016) 2529–2535.
- [25] K.K.I.U. Arunakumara, B.C. Walpole, M.H. Yoon, Banana peel: a green solution for metal removal from contaminated waters, *Korean J. Environ. Agric.*, 32 (2013) 108–116.
- [26] A.A. Najim, A.A. Mohammed, Biosorption of methylene blue from aqueous solution using mixed Algae, *Iraqi J. Chem. Petrol. Eng.*, 19 (2018) 1–11.
- [27] N. Feng, X. Guo, S. Liang, Y. Zhu, J. Liu, Biosorption of heavy metals from aqueous solutions by chemically modified orange peel, *J. Hazard. Mater.*, 185 (2011) 49–54.
- [28] Z. Kariuki, J. Kiptoo, D. Onyancha, Biosorption studies of lead and copper using rogers mushroom biomass '*Lepiota hystrix*', *S. Afr. J. Chem. Eng.*, 23 (2017) 62–70.
- [29] M.J. Nelson, G. Nakhla, J. Zhu, Fluidized-bed bioreactor applications for biological wastewater treatment: a review of research and developments, *Engineering*, 3 (2017) 330–342.
- [30] F. Tisa, A.A.A. Raman, W.M.A.W. Daud, Basic design of a fluidized bed reactor for wastewater treatment using fenton oxidation, *Int. J. Innovation Manage. Technol.*, 5 (2013) 93–98.
- [31] K.F. Ngian, W.R. Martin, Bed expansion characteristics of liquid fluidized particles with attached microbial growth, *Biotechnol. Bioeng.*, 22 (1980) 1843–1856.
- [32] G. Naja, B. Volesky, Behavior of the mass transfer zone in a biosorption column, *Environ. Sci. Technol.*, 40 (2006) 3996–4003.
- [33] T. Lin, L. Mingyan, H. Zongding, Hydrodynamics and adsorption mass transfer in a novel gas–liquid–solid circulating fluidized bed adsorber, *Ind. Eng. Chem. Res.*, 50 (2011) 3598–3612.
- [34] K. Kishore, N. Verma, Mass transfer study on counter current multi-stage fluidized bed ion exchanger, *Chem. Eng. Process. Process Intensif.*, 45 (2006) 31–45.
- [35] W. Yang, J. Wang, L. Zhou, Y. Jin, Gas–liquid mass transfer behavior in three-phase CFB reactors, *Chem. Eng. Sci.*, 54 (1999) 5523–5528.
- [36] A. Atta, S.A. Razzak, K.D.P. Nigam, J.X. Zhu, (Gas)–liquid–solid circulating fluidized bed reactors: characteristics and applications, *Ind. Eng. Chem. Res.*, 48 (2009) 7876–7892.
- [37] A.P. Mathews, I. Zayas, Particle size and shape effects on adsorption rate parameters, *J. Environ. Eng.*, 115 (1989) 41–55.
- [38] D.H. Sur, M. Mukhopadhyay, Process aspects of three-phase inverse fluidized bed bioreactor: a review, *J. Environ. Chem. Eng.*, 5 (2017) 3518–3528.
- [39] G. Bartelmus, Local solid–liquid mass transfer coefficients in a three-phase fixed bed reactor, *Chem. Eng. Process. Process Intensif.*, 26 (1989) 111–120.